I. Summary

In view of this report experiments were done with glass beads and coffee powder. The experiments were carried out with the Jenike Shear Cell and the Ring Shear Cell.

The experiments with glass beads were carried out with monosized particle samples to see if the particle size distribution has an influence on the flow behaviour. It turned out that the flow behaviour of glass beads is independent of the particle size distribution.
The measurements on coffee powder were more general. The goal was to get more information about the interesting flow behaviour or the coffee powder. During the experiments it became clear that coffee powder behaves very different as compared to other materials.
Due to the dimensions of the Jenike Shear Cell the stationary flow could not totally be reached. This resulted in unreliable data for the shear curves, because preshear had to be stopped too early. The preshear curves though could be used for analysis. After the initial increase of shear force all preshear curves increased with the same rate and all the data could be fitted by one model.
Also measurements were done on the density of the coffee powder. No exceptional things were discovered here. During preshear and shear the density of the sample increased and during relaxation it decreased again.
With the Ring Shear Cell some extra measurements were done to see if the stationary flow could be reached after longer shear. Due to the fact that the results of the Ring Shear Cell were not reproducible no real conclusions can be taken from this data. It seemed though that the result of the Ring Shear Cell and the Jenike Shear Cell were comparable.

Contents

1. Introduction

Most people think that coffee is a very well known material. They drink it every day, there are different aroma's and a lot of information is available about how to make coffee out of the coffee beans. Also the addictive part of coffee, caffeine is well examined.
So what is the goal of these experiments then? In the examples above the focus is on the chemical properties of coffee. In the experiments carried out in view of this report the focus is on the flow properties of the grind powder. In this research area there are still many questions in relation to coffee particles. Properties like flow behaviour, strain and stress seemed never very interesting, but in the last couple of years it turned out that understanding and control of these properties would be very interesting. The quality of the coffee particles can be a result of the forces (stress and strain) which acted on the particles during the production process. That is why a closer look is taken on the flow behaviour of the coffee particles. The questions posed are: How does coffee powder react to stress, compression and shear.

Coffee powder is a very peculiar granular material. In figure 1.1 a microscopic image of coffee particles can be seen. A closer look on the powder shows that the powder is a mixture of coffee particles which vary much in shape and size. The sizes of the coffee particles vary from a few microns to over a millimetre. The shape of the particles shows very rough edges, but there are also parts where the particle has an almost smooth surface.

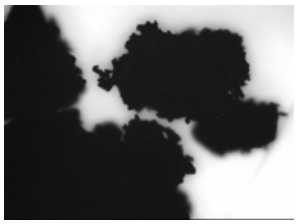

Figure 1.1: Coffee particles magnified (50x)

During the experiments, presented below, the goal was to learn more about the flow behaviour of coffee powder and about the characteristics of the material. These properties are mostly used to design equipment for storage, transportation or general handling of the bulk material. In the case of the coffee particles it also seems that the forces working on the coffee during the process influence the quality and therefore the taste of the coffee.
During earlier compression tests [1] it became clear that coffee behaves not like many other "normal" materials. The oils and other organic components inside a coffee particle seem to have an influence on the flow behaviour of coffee powder.

This project consists of three parts. First the characteristics of limestone were determined with the Jenike Shear Cell to get familiar with the device (not included in the report). After that the characteristics of glass beads with different monosized distributions were determined to see if size has an influence on the flow behaviour and finally it was attempted to characterise the flow behaviour of coffee powder. The characterisation of coffee powder was done with two devices, the Jenike Shear Cell and the Ring Shear Cell.

2. Shear Devices and Theory

During the experiments three different devices were used: the Jenike Shear Cell with computer, the Jenike Shear Cell with recorder and the Ring Shear Cell.
The Jenike Shear Cell with recorder was only used for the introduction measurements on limestone and is in principal the same as the Jenike Shear Cell with computer; that is why there will be only a description of the Jenike Shear Cell with computer.

2.1 The Jenike Shear Cell

The Jenike Shear Cell is used to measure the flow behaviour of materials. With the Jenike device the stationary flow and the characteristics of a material can be measured. The device used also had laser sensors to measure the volumetric strain of the sample and had a maximum shear distance of 8 mm.
In figure 2.1 and 2.2 schematic drawings of the Jenike Shear Cell can be seen. The shear cell consists of a base, a shear ring and a shear lid. The shear lid itself has a bracket and a pin.

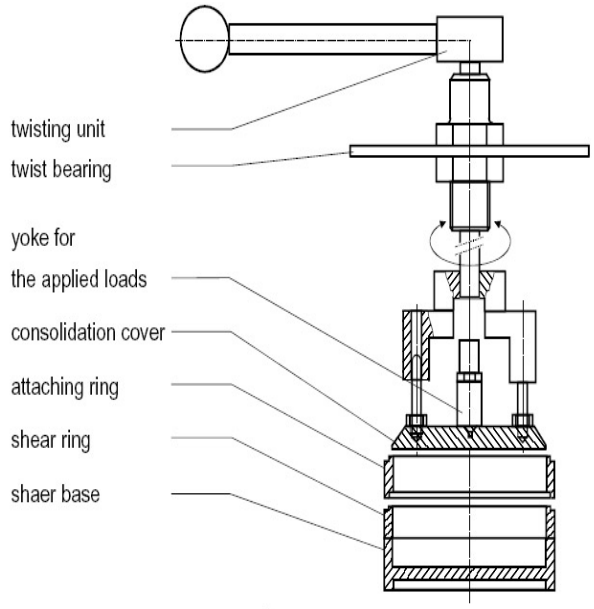

Figure 2.1: Schematic drawing of the Jenike Shear Cell

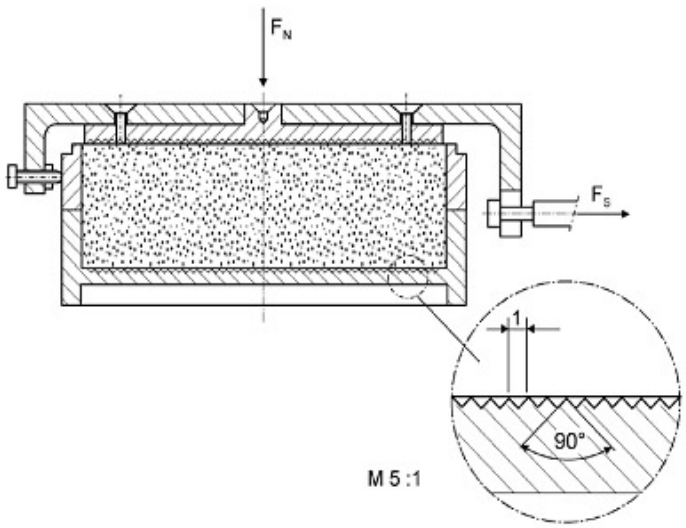

Figure 2.2: Shear Cell of the Jenike Shear Cell

During shear several forces will be applied to the sample. There is the normal force (F_N) which is applied by a weight hanging from the top of the shear cell and there is a shear force (F_S), applied by a motor which pushes the upper ring to create a shear plane in the sample.
In table 2.1 and table 2.2 the dimensions of the Jenike Shear Cell are summarized.

Table 2.1: General information of the Jenike Shear Cell

Shear cell	256.6	g
Shear base	196.2	g
Shear ring	60.4	g
Top for twisting	0.2	kg
Top for shearing	0.13	kg
Big yoke	1.21	kg
Small yoke	0.19	kg
Shear speed	2.00	mm/min

Table 2.2: Dimensions of the Jenike Shear Cell

Diameter	D	0.095 m
Height of the base	h_B	0.016 m
Height of the ring	h_R	0.014 m
Volume of the base	V_B	$1.13*10^{-4}$ m^3
Volume of the ring	V_R	$9.92*10^{-5}$ m^3
Shear area	A	0.007 m^2
Rate of fall	g	9.81 m/s^2

The normal stresses applied in the experiments were determined following table 2.3 and 2.4 (table 1 and 2 from [2]). From the experiments with different normal stresses, shear stresses can be obtained. A plot of the shear stress versus the normal stress gives a yield locus. In figure 2.3 a schematic of a yield locus can be seen. Tangential to this yield locus a stress circle (B2), also called Mohr-circle, can be drawn. The Mohr-circles represent a stress state where the bulk solid starts to flow. Circles beneath the yield locus (B1) can only cause a plastic deformation, while circles above the yield locus cannot occur, because the sample breaks under the conditions needed.

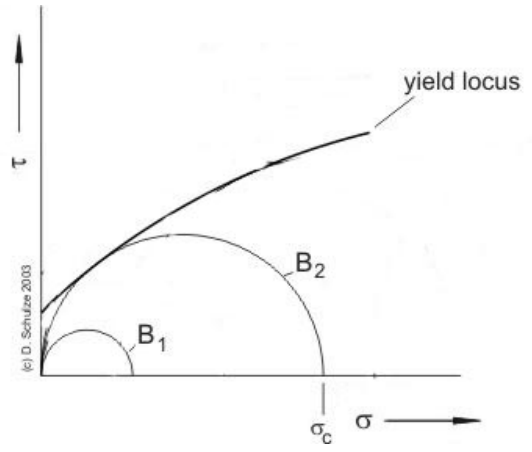

Figure 2.3: Schematic of a yield locus and a Mohr-circle

Table 2.3: normal stresses at preshear ($\sigma_{An,i}$)

$\rho_{b,0}$	$\sigma_{An,i}$ (in kPa)			
kg/m³	YL 1	YL 2	YL 3	YL 4
< 300	1.5	3	6	12
300 … 800	2	4	8	16
800 … 1600	2.5	5	10	20
1600 … 2400	3	6	12	24
> 2400	4	8	16	32

Table 2.4: normal stresses at shear ($\sigma_{Ab,i}$)

σ_{ab1} =	0.25 · $\sigma_{An,i}$
σ_{ab2} =	0.40 · $\sigma_{An,i}$
σ_{ab3} =	0.60 · $\sigma_{An,i}$
σ_{ab4} =	0.80 · $\sigma_{An,i}$

The normal stress can be converted to normal load with formula (2.1).

$$m_N = \frac{\sigma_i \cdot A}{g} - m_J - m_D - m_R - V_R \cdot \rho_b \qquad (2.1)$$

The Jenike Shear Cell is operated by the standard operation sequence below.

Operation sequence of the Jenike Shear Cell:

1. Fill the powder in the shear cell taking an appropriate consolidation ring
2. Apply preconsolidation and twisting with a high consolidation load
3. If the surface of the powder is beneath the top of the upper ring, fill the ring with up with fresh powder and apply again preconsolidation. Otherwise excess material is scraped level with the top of the mould ring
3. Lower the load to the preshear load
4. Position the laser sensors above the shear lid
5. Start the measurement procedure on the PC
6. Preshear (Preferably until both the shear force and the volumetric strain curves show the stationary behaviour)
7. Unloading
8. Change the load to the shear load
9. Start shear
10. Stop the motor
11. Unloading
12. Stop the measurement procedure on the PC
13. Measurement evaluation with ARGUS
14. Weigh the shear cell with powder

This operation sequence is carried out for different preconsolidation forces, preshear and shear forces.

After the measurements the data obtained can be analysed. To analyse the data the normal stress and the shear stress have to be calculated. This can be done by formula (2.2) and (2.3).

$$\sigma = (m_N + m_J + m_D + m_R + V_R \cdot \rho_b)\frac{g}{A}. \quad (2.2)$$

Here is m_N the weight of the normal load, m_j weight of the yoke, m_D the weight of the cover, m_R the weight of the ring, V_R the volume of the ring and ρ_b the density of the sample. The volume of the ring times the density is taken into account in the measurements below, but is actually neglectable.

$$\tau = \frac{F_S}{A} \quad (2.3)$$

2.2 The Ring Shear Cell

For another serie of experiments the Ring Shear Cell was used. The Ring Shear device can measure the flow behaviour of powders over large shear displacements. The advantage of this device is that it can shear for practically an infinite time, because it shears in a circle.

The Ring Shear Cell can be seen in pictures 2.4 and 2.5 and the dimensions of the cell are summarised in table 2.5.

Table 2.5: Dimensions of the Ring Shear Cell

Outer shear cell diameter	D_a	255 mm
Inner shear cell diameter	D_i	154 mm
Lever arm diameter	D_H	326 mm
Shear area	A_Z	324.44 m^2
Inner height	h_T	47 mm
Cover weight	m_D	3.0 kg

Figure 2.4: Ring Shear Cell

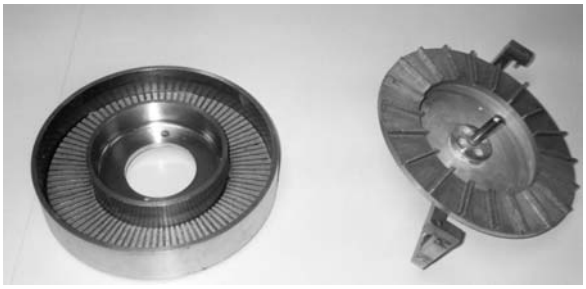

Figure 2.5: Shear base and top of the Ring Shear Cell

In the Ring Shear Cell the normal stresses are applied by a hydraulic cylinder. The hydraulic pressures used are given in table 2.6. The pressures for yield locus 1, 2 and 3 were too small to apply. That is why only yield locus 4 and a new yield locus, yield locus 5, were measured.

Table 2.6: preshear and shear pressures

Yield locus 4		**Yield locus 5**	
Preshear (bar)	Shear (bar)	Preshear (bar)	Shear (bar)
2.86	1.00	5.95	1.31
	1.62		2.24
	2.24		3.48
			4.70

Procedure for preshear and shear

1. The material is filled loosely into the shear cell base and the cover is put on the sample.
2. The preshear stress is applied by the hydraulic pressure and the shear cell is rotating until the shear force (F_S) has reached the stationary flow regime.
3. The direction of the shear cell is reversed until the shear force is zero. The rotation of the shear ring is stopped and the hydraulic cylinder is lifted
   from the cell, the preshear stress is changed to the shear stress and the hydraulic cylinder is pushed down again.
4. Shear into shear direction until the shear force has reached its maximum value.
5. Change direction of the shear cell again until the shear force is zero. Lift the hydraulic cylinder, change the shear stress to the preshear stress and pull the hydraulic cylinder down.
6. Rotate the cell in shear direction until the shear force F_S is constant again.
7. Repeat step 3 to 6 until there are enough measured points.

The results of the Ring Shear Cell are evaluated with the program ARGUS on the computer.

In principle the theory behind the Ring Shear Cell is the same as behind the Jenike Shear Cell. Only in the Ring Shear Cell the shear stress is applied by a hydraulic cylinder and the shear plane is in a circle. For the Ring Shear Cell work formulas (2.4) and (2.5) can be derived. These formulas are derived respectively from formula (2.2) and (2.3). In appendix A the derivations are included.

$$\sigma[kPa] = p_{hydr}[bar] * 3.88 + 0.91[kPa] \quad (2.4)$$

$$\tau\,[kPa] = (F_{s,1} + F_{s,2})\,[N] * 1.57/32.4[1/m^2] \quad (2.5)$$

The largest difference between the Jenike Shear Cell and the Ring Shear Cell is that the Ring Shear Cell can shear for an infinite time and length. Therefore preconsolidation is not necessary in the Ring Shear Cell.

3. Results

Measurements are performed on glass beads and coffee powder, both granular materials. The experiments on glass beads are done to see if a relation exists between particle size and shear stress. For coffee powder experiments were performed to get more information on the flow behaviour. Especially on how coffee powder reacts to stress, compression and shear.
In section 3.1 the results obtained for glass beads are discussed and in section 3.2 the results for coffee powder.

3.1 Glass beads

The experiments with glass beads were carried out with different samples of monosized and bisized particles to see if there is a relation between particle size and shear stress. The glass beads used had a density of $1.5*10^{3}$ $^{kg}/_{m}^{3}$. All measurements were carried out with the Jenike Shear Cell.

In table 3.1.1, below, the different samples are listed.

Tablel 3.1.1: particle range of different size distributions

sample	particle range (µm)
A	160-250
B	230-320
C	400-520
D	690-750
E	Mix of A and D
F	Mix of C and D

For the each of the samples three different yield loci were measured. Only for sample B one yield locus was measured.
In the first couple of experiments the samples were twisted 40 times during preconsolidation, but it turned out that twisting did not have any effect on the results and that it only broke the glass beads. In the rest of the measurements was decided to twist only 1 time during preconsolidation. This one twist was necessary to rearrange the particles in a nice plane inside the shear cell. Microscopic pictures of the glass beads afterwards showed no (obvious number of) broken glass beads (see figure 3.1.1 and figure 3.1.2 for a representative example), so it was justified to re-use the glass beads during the experiments. The experiments were carried out as described in section 2.1.

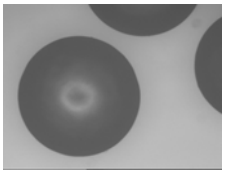

Figure 3.1.1: sample D before experiments

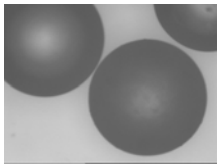

Figure 3.1.2: sample D after experiments

For every size distribution the shear stress was measured at different yield loci. The consolidation stress (σ_C), normal stress at preshear (σ_{pr}) and the normal stress at shear (σ_{sh}) were determined according to table 2.3 and table 2.4. In table 3.1.2 the different yield loci can be seen. The measurements were carried out in the following sequence: σ_3, σ_2, σ_1, σ_2, σ_1, σ_3.

Table 3.1.2: consolidation stress (σ_C), normal stress at preshear (σ_{pr}) and the normal stress at shear (σ_{sh}) for different yield loci

Measurement	Yield locus	σ_C (kPa)	σ_{pr} (kPa)	σ_{sh} (kPa)
1.1	1	7.5	2.5	0.7
1.2			2.5	1.3
1.3			2.5	2.0
2.1	2	12.5	5.0	1.3
2.2			5.0	2.5
2.3			5.0	4.0
3.1	3	20.0	10	2.5
3.2			10	5.0
3.3			10	8.0

Of each of the samples A, C and D three different yield loci were determined. The results of all the measurements can be found in appendix B. In figure 3.1.3 the representative results for size distribution D at yield locus 3 are shown.
The different lines in the graph indicate the different experiments. The first plateau in the graph indicates shear force at preshear. This force has a maximum and a slight increase. This force is the force at which stationary flow occurs. The second plateau indicates the maximal force at shear. These maximal forces are measured for different normal forces. (See table 3.1.2.) The consolidation stress and the normal stress at preshear was for all experiments at this yield locus the same and every normal stress at shear was measured twice.
For size distribution A and B the results showed a little bit of scattering. An explanation for the scattering is that the particles were very small and they got between the shear base and the shear ring of the Jenike Shear Cell during the experiments. For samples C, D, E and F the particles were big enough and no scattering was seen.

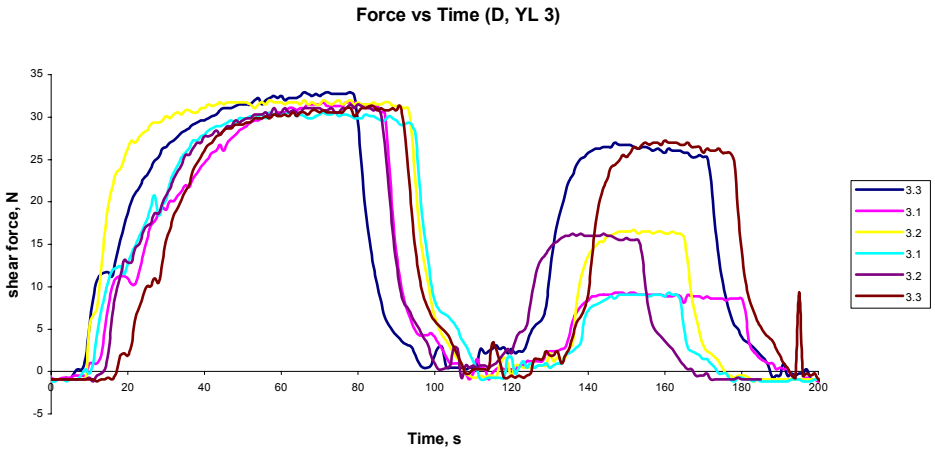

Figure 3.1.3: Force versus time for glass beads with size distribution D

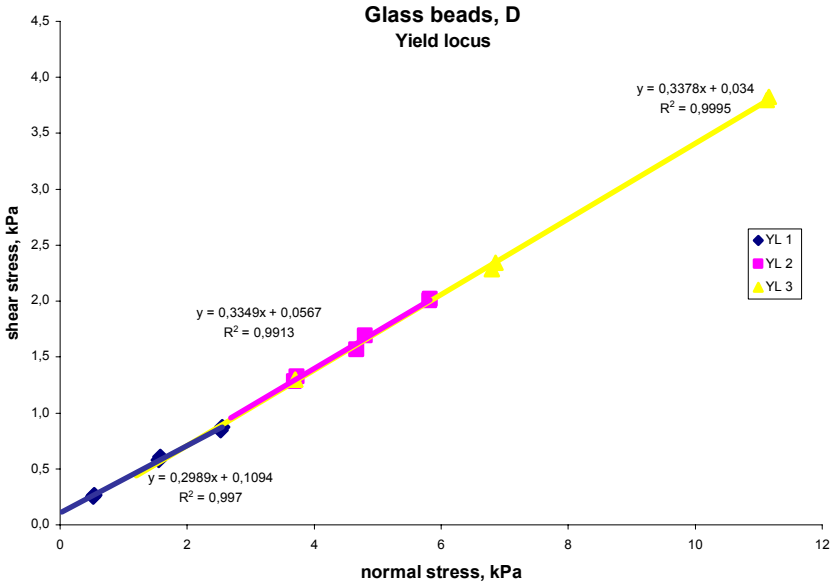

Figure 3.1.4: τ plotted against σ for the three different yield loci measured with size distribution D

The maximal force at shear is related to the shear stress (τ) (see formula (2.3)). With the shear stress known, a graph can be made of the yield locus. In figure 3.1.4 such a graph can be seen for the three measured yield loci at size distribution D.
From the figure it is clear that the slope is independent of the yield loci, as all lines have the same slope, within the uncertainty. All three lines also have a small intersection with the y-axis near zero (intersections are between 0.03-0.1). This intersection is a measure of the cohesion. A cohesion near zero indicates a free flowing behaviour of the glass beads.
In figure 3.1.5 the yield loci are forced through zero. The deviation from the measured points, R-squared, is slightly bigger than in figure 3.1.4, but is still acceptable. In appendix B similar graphs can be seen for all size distributions. The glass beads seem to have a free flowing behaviour for all sizes examined. Visually it can also be seen that the glass beads behave freely flowing. So it is save to say that the glass beads are a free flowing, almost cohesionless material.

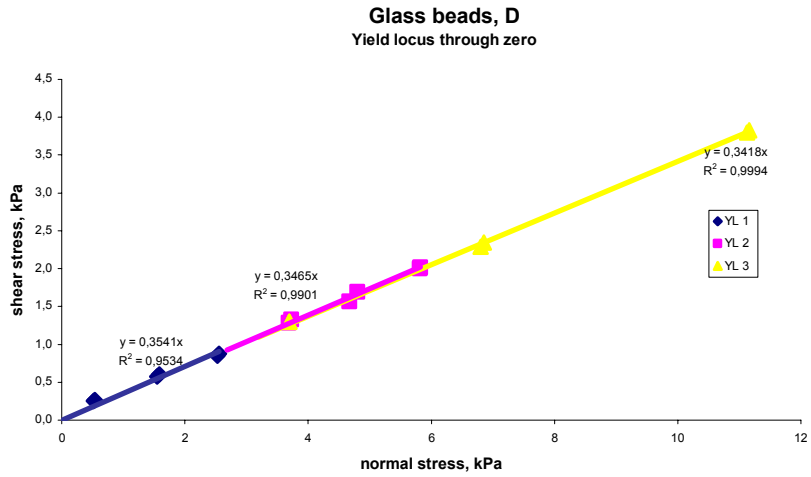

Figure 3.1.5: τ versus σ for the three different yield loci measured at size distribution D forced through zero

After the measurements on monosized distributions, measurement were also performed with mixtures of two monosized distributions. Distribution E was a mixture of distributions A and D. In sample E1 was 90 weight-% of A present and 10 weight-% of D. In sample E2 was 50 weight-% of A and 50 weight-% of D present. Distribution F was a mixture of distributions C and D. Here were also two different samples. Sample F1 contained 75 weight-% of C and 25 weight-% of D and sample F2 consisted of 65 weight-% of C and 35 weight-% of D.
Figure 3.1.6 shows a graph with shear stress versus normal stress for distribution E and figure 3.1.8 shows the same graph, but for distribution F. From both figures it is clear that the results obtained from the mixtures do not deviate much from those obtained from the pure distributions. In graphs 3.1.7 and 3.1.9 the fitted lines are forced through zero. One remark is that all results are very close to each other, even the results of distribution A and distribution D, so it is hard to say if there is a difference at all between the different size distributions.

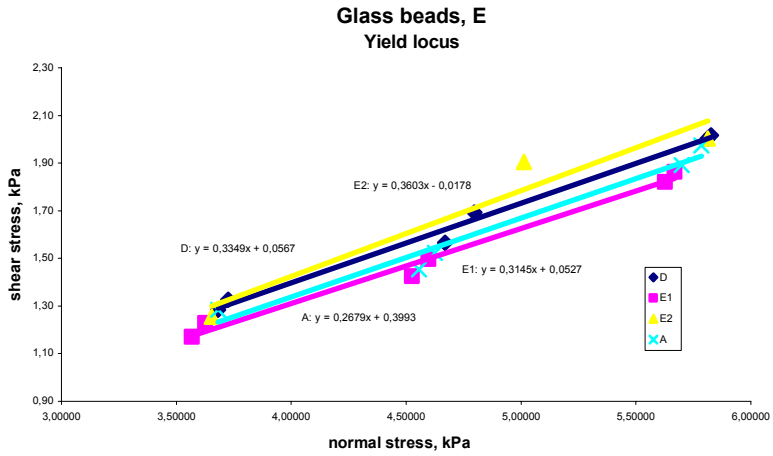

Figure 3.1.6: τ versus σ for yield loci 2 measured at size distributions A, D, E1 and E2

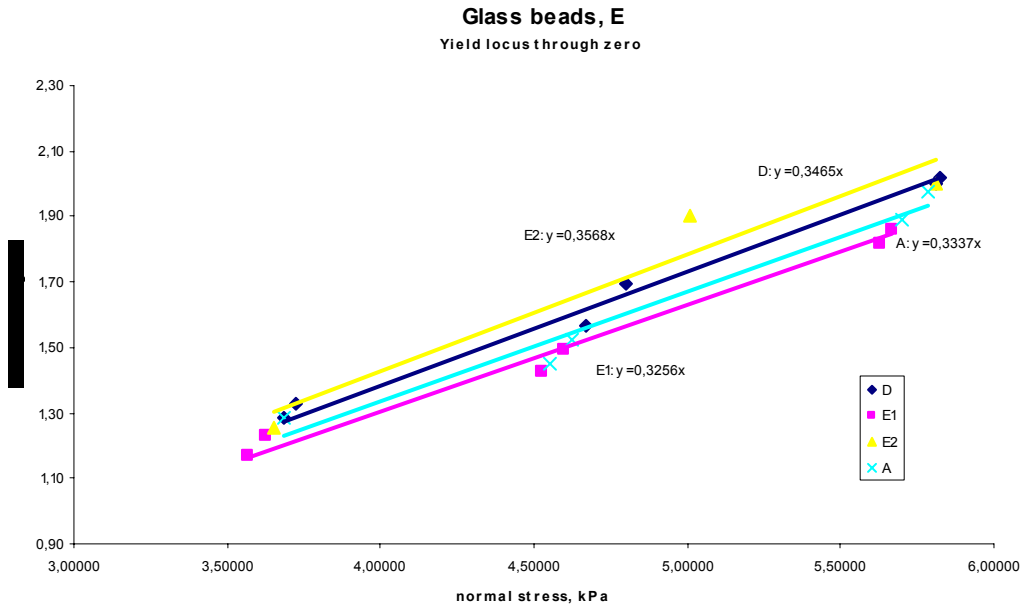

Figure 3.1.7: τ versus σ for yield loci 2 measured at size distributions A, D, E1 and E2 forced through zero

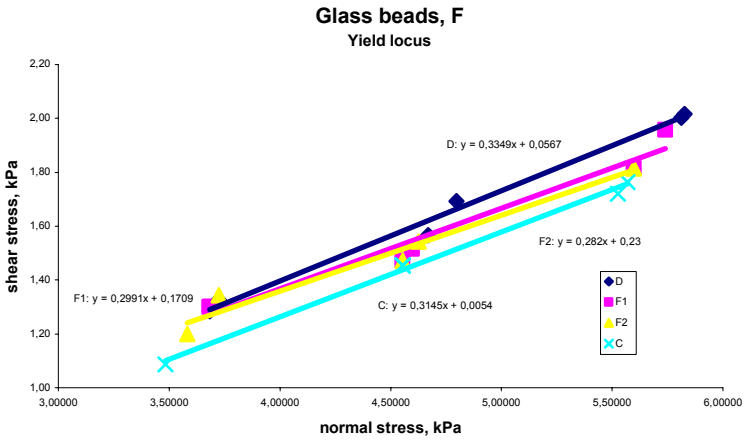

Figure 3.1.8: τ versus σ for yield loci 2 measured at size distributions A, D, F1 and F2

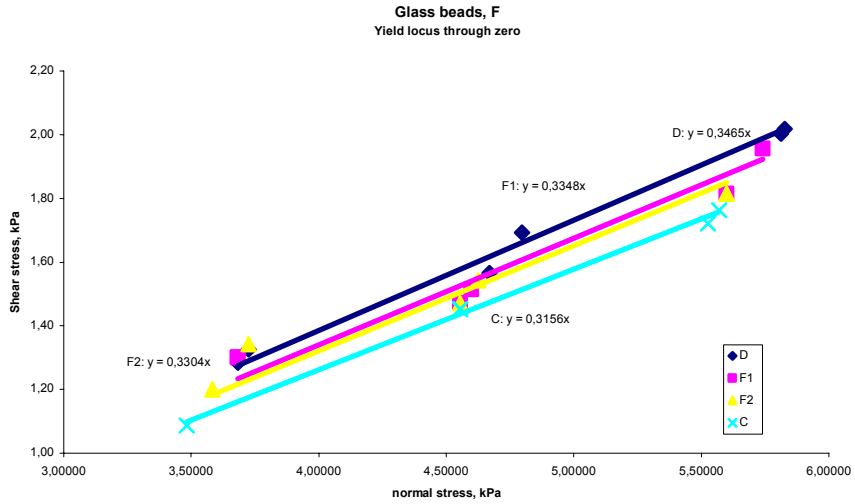

Figure 3.1.9: τ versus σ for yield loci 2 measured at size distributions A, D, F1 and F2

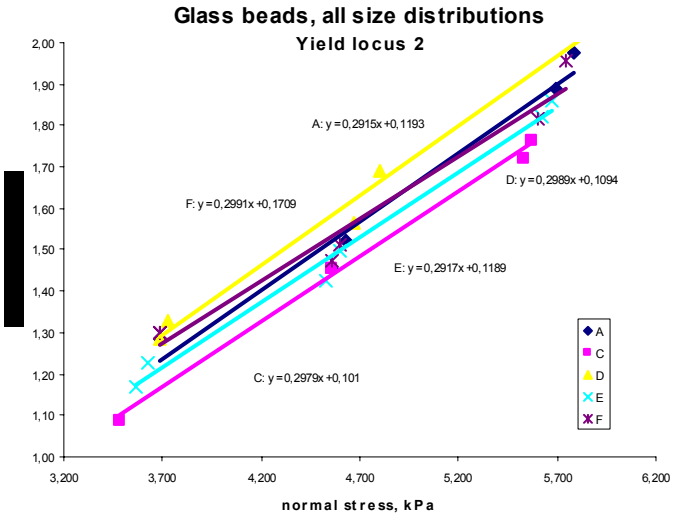

Figure 3.1.10: τ versus σ for all size distributions at yield locus 2

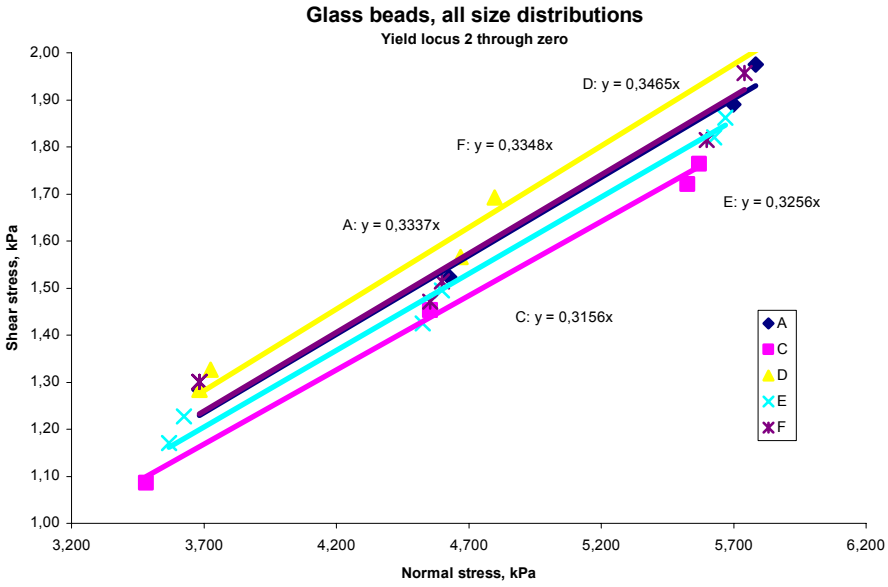

Figure 3.1.11: τ versus σ for all size distributions at yield locus 2 forced through zero

Table 3.1.3: parameters for equations of the different particle size distributions at yield locus 2

Equation: $\tau = a\sigma + \mu$

Size distribution	a (-)	μ (kPa)
A	0.2915	0.1193
C	0.2979	0.101
D	0.2989	0.1094
E	0.2917	0.1189
F	0.2991	0.1709

Table 3.1.4: parameter for equations of the different particle size distributions forced through zero at yield locus 2

Equation: $\tau = b\sigma$

Size distribution	b (-)
A	0.3337
C	0.3156
D	0.3465
E	0.3256
F	0.3448

To see what the influence of different particle sizes on the stress is we have to take a look at one yield locus for the different particle size distributions. In figure 3.1.10 and 3.1.11 size distributions A, C, D, E and F are plotted in one graph for yield locus 2 and in table 3.1.3 and 3.1.4 the corresponding fit equations of the lines can be seen. From the table it is clear that all equations are the same, within the limits of uncertainty. The general formula for the glass beads is $y = 0.29x + 0.1$ when the data is not forced through zero and $y = 0.33x$ when it is forced through zero.

From these results, described above, several things can be concluded. It is clear that glass beads is a free flowing material, that means a cohesionless material and the shear stress of glass beads is independent of particle size. More general can be said that the shear stress is independent of particle size for spherical, granular, hard materials. Another granular material is coffee powder. Coffee powder is like glass beads a granular material, but it is not as spherical and hard as glass beads. Coffee powder is a soft material and most of the particles are non-spherical. Another difference between glass beads and coffee powder is the particle size distribution. Is this distribution for glass beads nicely monosized for coffee the powder is always a mixture of different particle sizes. Although there are a lot of differences between glass beads and coffee powder, they are still both granular materials. That is why in the next section for coffee powder is assumed that the particle size distribution has no influence on the results.

3.2 Coffee powder

For the experiments on the organic, everyday material, coffee, coffee powder of the Dutch brand Douwe Egberts was used. The powder had a bulk density of 267 $^{kg}/_{m}{}^{3}$, measured before consolidation. The coffee particles were tested with the Jenike Shear Cell and the Ring Shear Cell to obtain information about compression, shear and stress. First the experiments with the Jenike Shear Cell will be discussed and after that the results of the experiments with the Ring Shear Cell

3.2.1 The Jenike Shear Cell

With the Jenike Shear Cell three different yield loci of the coffee powder are measured. The yield loci were again determined according to table 2.3 and table 2.4. As can be seen in table 3.2.1 yield loci 2, 3 and 4 are measured. Yield locus 1 is not measured, because the stresses needed for this yield locus were too small for the device. In table 3.2.1 the yield loci, consolidation stress (σ_C), normal stress at preshear (σ_{pr}) and normal stress at shear (σ_{sh}) can be seen. Every measurement is carried out twice in the following sequence: σ_3, σ_4, σ_2, σ_1, σ_2, σ_4, σ_1, σ_3.

Table 3.2.1: consolidation stress (σ_C), normal stress at preshear (σ_{pr}) and the normal stress at shear (σ_{sh}) for different yield loci

Measurement	Yield locus	σ_C (kPa)	σ_{pr} (kPa)	σ_{sh} (kPa)
c1.1	2	7.5	3.0	0.75
c1.2				1.2
c1.3				1.8
c1.4				2.4
c2.1	3	12.0	6.0	1.5
c2.2				2.4
c2.3				3.6
c2.4				4.8
c3.1	4	12.0	12.0	3.0
c3.2				4.8
c3.3				7.2
c3.4				9.6

Appendix C shows for every yield locus the time versus shear force diagrams. In figure 3.2.1 the diagram of yield locus 4 can be seen. The first part of the curves, to approximately 250 s, shows the shear force as a result of the normal stress at preshear. For reliable data on maximal shear force at shear, the shear force during preshear has to reach a steady value. From the graph(s) it is not clear if this stationary flow is reached or almost reached. Longer application of the preshear was not possible, because the shear base used, allows only 8 mm of shear, which was clearly too short to see if steady flow was reached. The second part of the curves show the shear force during shear.

At the beginning of some of the curves a ‘failure’ peak can be seen. This failure peak can be a material property. The problem with the coffee powder is that not in every curve a failure peak is found. Several values are compared with each other, but is seemed that none of the properties looked at was an explanation for the occurrence of the peaks. A possible explanation can be that the failure peak only occurs after a certain time of preconsolidation. Unfortunately the time of preconsolidation was not systematic and was not measured so that nothing can be said about the occurrence of the failure peaks.

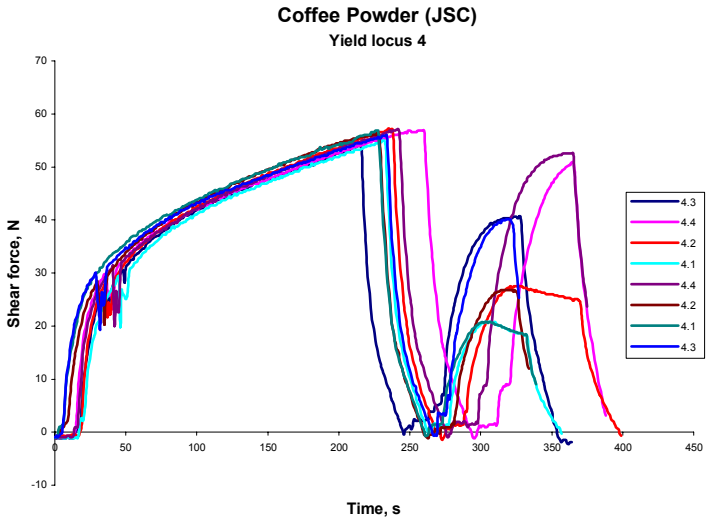

Figure 3.2.1: Shear force versus time for yield locus 4, measured with the Jenike Shear Cell

Although it is not clear if stationary flow is reached during preshear, the curves of preshear still can be compared with each other, because every preshear curve is a result of shearing for more or less the same time. One thing that can be determined from the measurements is a graph of the shear stress, τ, versus normal stress, σ, for the different yield loci. This graph can be seen in figure 3.2.2. The curves of the three yield loci are parallel lines with a slope of about 0.4. The intersection with the y-axis is for the lines of yield locus 2 and 3 close together, but for yield locus 4 it is clearly a higher value. It can be that there is a kind of threshold in the flow behaviour of coffee powder. This threshold can be caused by the oils in the powder. For the lower weights the force on the sample is to small to push these oils out of the coffee particles, but for the higher weight at yield locus 4 it can be that these oils are pushed out of the particles and have an influence on the flow behaviour. The value of the cohesion, as compared to the stress levels, is a confirmation that coffee is not a free flowing material, but also not a very sticky one.

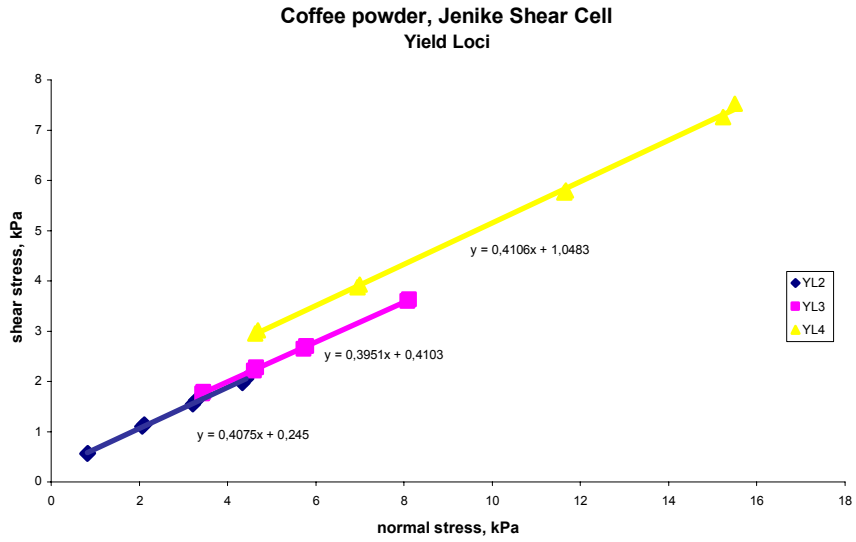

Figure 3.2.2: shear stress, τ, versus normal stress, σ, for the different yield loci of coffee powder

To get better information out of the measurements, the shear forces were converted to results independent of the applied normal stresses. This is done by converting the shear force to shear stress (formula 2.3) and by dividing the shear stress by the normal stress applied. In figure 3.2.3. the first peaks of the dimensionless curves of the shear stress versus time can be seen. From this graph it is

clear that a higher yield locus results in a smaller shear stress ratio, but it looks like the curves have the same slope after about 40 seconds.

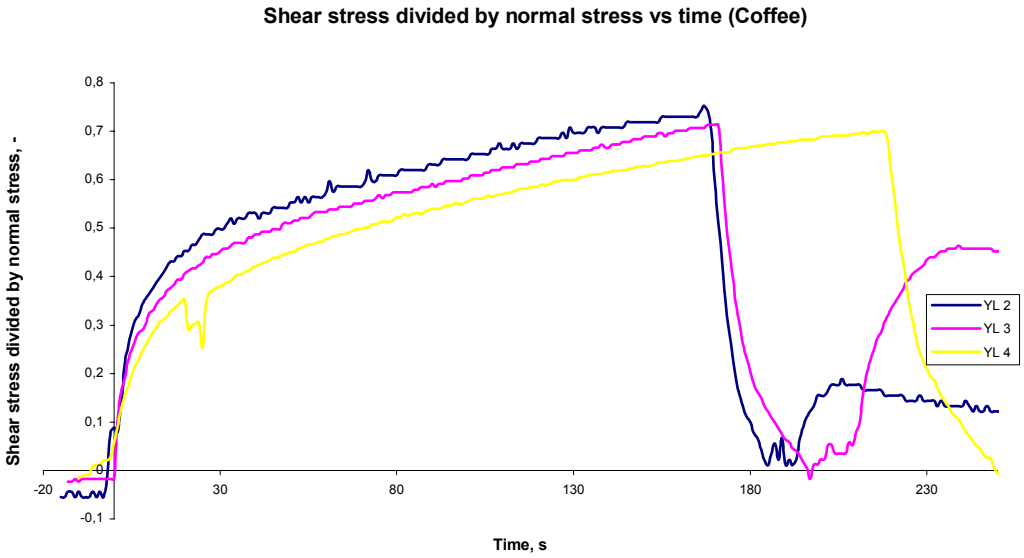

Figure 3.2.3: shear stress divided by normal stress versus time for the different yield loci of coffee

To see if the if the different measurements reach a curve with the same slope, a fit is made of all the measured curves. In table 3.2.2 the results of the fit are shown. The data is fitted to the model:

$$\tau/\sigma = c(x+x0)^{-A}$$

Where x is t/t_0 and x_0 is t_{00}/t_0. The fit was performed in the increasing part of the curves. The peaks of the curves were not included. In Figure 3.2.4 and 3.2.5 parameters c and A are plotted. Although the points, in both figures, are quite scattered, a nice line can be obtained through the data. The equations obtained for parameter c and parameter A are given in below in formula (3.1) and (3.2)

$$c = -0.0057\sigma + 0.2472 \qquad (3.1)$$

$$A = 0.0037\sigma + 0.2246 \qquad (3.2)$$

For parameter c the limitation holds that c has to be greater or equal to zero. This means that extrapolation in graph 3.2.4. gives a maximal normal stress of 43 kPa.

In earlier experiments [1] another function was found that described the flow behaviour. The function found there was:

$$f = f_{max} - (f_{max} - f_{\infty})[1-(1+t/t_0)^{-A}]$$

Table 3.2.2: results of the fitted data to the model $\tau/\sigma = c/(x+x0)^A$

measurement	Yield locus	σ_{pr} (kPa)	c (-)	x0 (-)	A (-)
262	2	5,355	0,1956	-19,0122	-0,26811
263	2	5,355	0,21775	-12,8925	-0,23302
264	2	5,469	0,244818	-16,1773	-0,23103
265	2	5,398	0,210874	-10,5519	-0,25118
268	2	5,355	0,228669	-13,0239	-0,22703
270	2	5,398	0,204458	-18,8633	-0,25078

271	2	5,398	0,233578	-17,2803	-0,22387
272	2	5,469	0,252972	-5,27639	-0,21964
252	3	9,915	0,14727	-19,9835	-0,30717
253	3	10,186	0,184866	-16,5327	-0,26387
254	3	10	0,14964	-20	-0,303
255	3	10,229	0,18131	-24,5771	-0,27516
256	3	10,186	0,217339	-21,4667	-0,23617
257	3	10,157	0,173048	-14,0324	-0,26852
258	3	10,143	0,179708	-18,9974	-0,26628
259	3	10,1	0,188237	-14,5755	-0,25663
275	4	17,819	0,150049	-20,5813	-0,28271
276	4	18,248	0,152029	-16,5096	-0,27989
277	4	18,248	0,137505	-19,0237	-0,30465
278	4	17,919	0,14032	-22,3957	-0,2946
279	4	18,248	0,144984	-16,4742	-0,29013
280	4	18,148	0,13534	-11,296	-0,30732
281	4	18,305	0,165741	-9,53081	-0,26582
282	4	18,148	0,150307	-8,44456	-0,28105

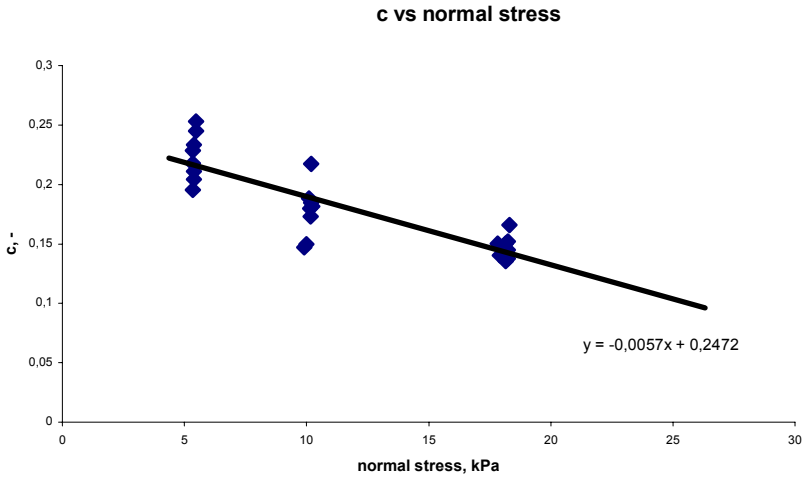

Figure 3.2.4: c versus normal stress for $\tau/\sigma = c/(x+x0)^A$

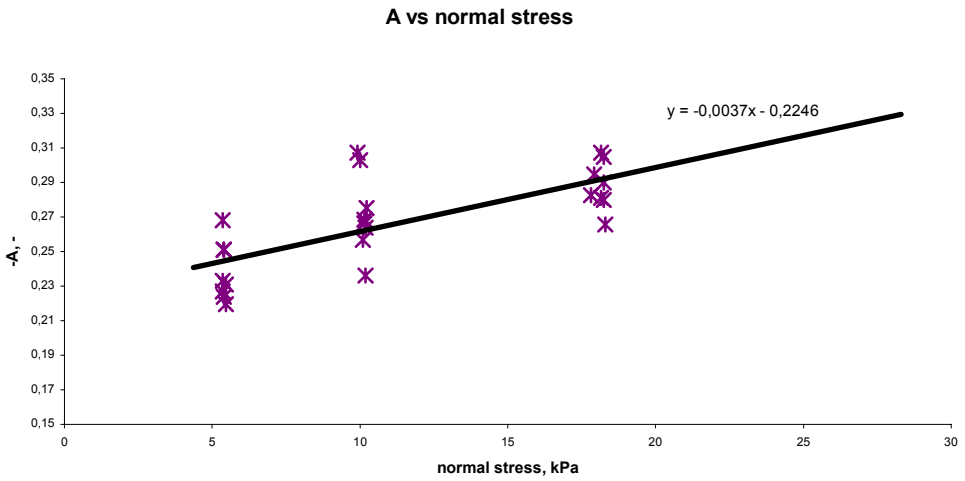

Figure 3.2.5: -A versus normal stress for $\tau/\sigma = c/(x+x0)^A$

Finally a closer look is taken at the volume of the sample during the measurements. Of every sample on four places the distance between the laser and the top of the shear cell is measured. In appendix C some graphs can be seen of height measurements. (Graphs C1.6-C1.8.) From this graphs it is clear that no big difference between the heights measured with the four different laser, which would indicate a tilt of the top, so it is safe to take the average value of the heights.
The height curves of graphs C1.6-C1.8 can be converted to volumetric strain curves. This can be done with the following formula:

Volumetric strain = -(d-d*)/160

Here is d the distance between the lasers and the top of the cell and d* the same distance, but at the start of the measurement. An example of a volumetric strain curve can be seen in figure 3.2.6. In graph 3.2.7. the volumetric strain curve is combined with a shear force curve. From this graph it can clearly be seen that the steep decrease of the volumetric strain, around 200 seconds, occurs at the moment that preshear stress is removed from the sample. When the shear stress is applied the volumetric strain increases again and the last decrease is again due to the release of the stress.

In graph 3.2.6. four ‘peaks’ can be seen. One at 30 seconds, one at 160 seconds, one at 200 seconds and one at 260 seconds. For every measurement these peaks are collected in table 3.2.3. Peak 1 and 2 are measured during pre shear and peak 3 and 4 are measured during shear.

In figure 3.2.8 the four peaks are plotted against normal stress. Here it can be seen that the curve of peak 1 has an intersection with the curve of peak 2. This intersection is the point at which maximal dilatancy is reached and after which only compression occurs. So above a normal stress of 25 kPa only compression of the coffee takes place.
The differences between the peaks are shown in figure 3.2.9. These differences indicate the different paths during the shear process. Peak 1 minus peak 0 (taken as zero) indicates the initial dilatancy before shear can occur. Peak 2 minus peak 1 indicates compression during preshear, peak 3 minus peak 2 indicates dilatancy due to release of the preshear and finally peak 4 minus peak 3 indicates compression during shear. From figure 3.2.9 some important numbers can be derived. The intersection of the line given by peak 1 minus peak 0 with the x-axis is a measure for the normal stress needed before compression occurs. Compression occurs from 0.8 kPa.

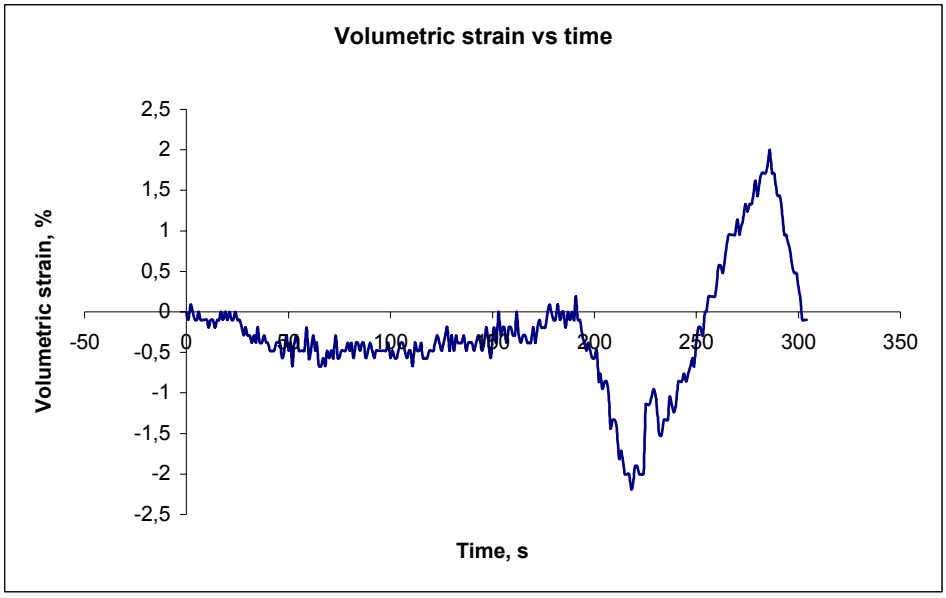

Figure 3.2.6: Volumetric strain versus time, yield locus 3

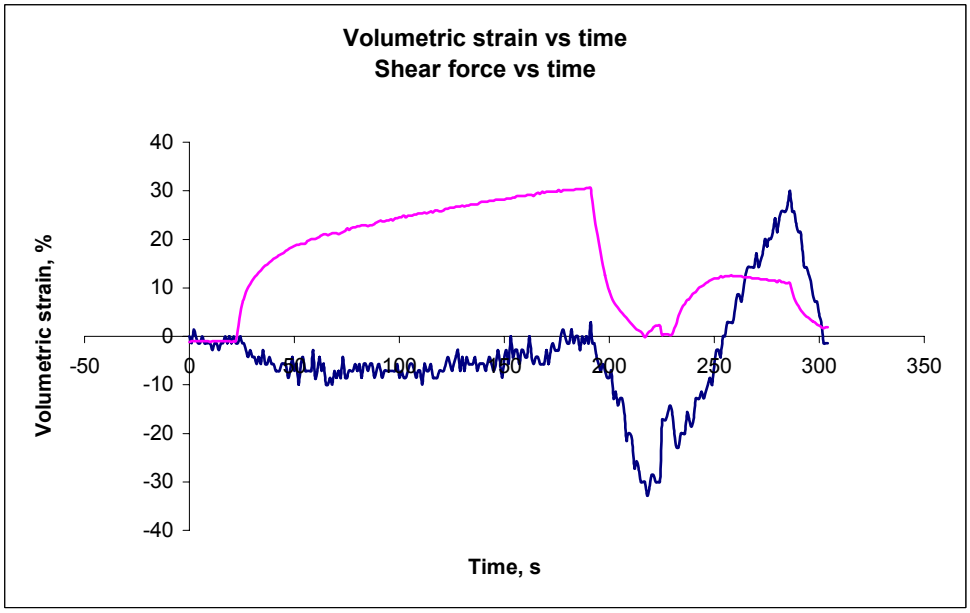

Figure 3.2.7: Distance between the top of the shear cell and the lasers together with a shear curve for yield locus 3

Table 3.2.3: values of the volumetric strain peaks for all measurements

Yield locus	σ_{pr} (kPa)	measurement	Peak 1	Peak 2	Peak 3	Peak 4	Peak 2-Peak 1	Peak 3–Peak 2	Peak 4- peak 3
2	5,355	262	-0,38	0,57	-1,48	1,81	0,95	-2,05	3,29
2	5,355	263	-0,57	0,38	-1,52	0,47	0,95	-1,9	1,99
2	5,469	264	-0,47	1,42	-0,66	3,34	1,89	-2,08	4
2	5,398	265	-0,76	0,28	-1,43	2,57	1,04	-1,71	4
2	5,355	268	-0,38	0,38	2	-0,095	0,76	1,62	-2,095
2	5,398	270	-0,57	0,38	-1,62	1,62	0,95	-2	3,24
2	5,398	271	-0,57	0,19	-1,33	3,43	0,76	-1,52	4,76
2	5,469	272	-0,28	0,95	-0,76	2,19	1,23	-1,71	2,95
3	9,915	252	-0,57	-0,19	-2,1	0,38		-1,91	2,48
3	10,186	253	-0,66	-0,28	-2,57	-0,76	0,38	-2,29	1,81
3	10	254	-0,85	-0,096	-2,19	0,66	0,754	-2,094	2,85
3	10,229	255	-0,66	0,095	-2,09	2	0,755	-2,185	4,09
3	10,186	256	-0,76	-0,095	-2,19	0,47	0,665	-2,095	2,66
3	10,157	257							
3	10,143	258	-0,57	-0,095	-2	1,14	0,475	-1,905	3,14
3	10,1	259	-0,85	-0,38	-2,57	0,28	0,47	-2,19	2,85
4	17,819	275	-1,62	-1,52	-4	-1,24	0,1	-2,48	2,76
4	18,248	276	-1,42	-0,76	-3,71	-1,52	0,66	-2,95	2,19
4	18,248	277	-1,52	-1,05	-3,53	0,85	0,47	-2,48	4,38
4	17,919	278	-1,91	-1,61	-4,4	-0,47	0,3	-2,79	3,93
4	18,248	279	-1,81	-1,33	-4,19	-1,43	0,48	-2,86	2,76
4	18,148	280	-1,71	-1,33	-4	-1,24	0,38	-2,67	2,76
4	18,305	281	-2	-1,62	-4,48	-0,19	0,38	-2,86	4,29
4	18,148	282	-1,61	-1,14	-3,9	-1,72	0,47	-2,76	2,18

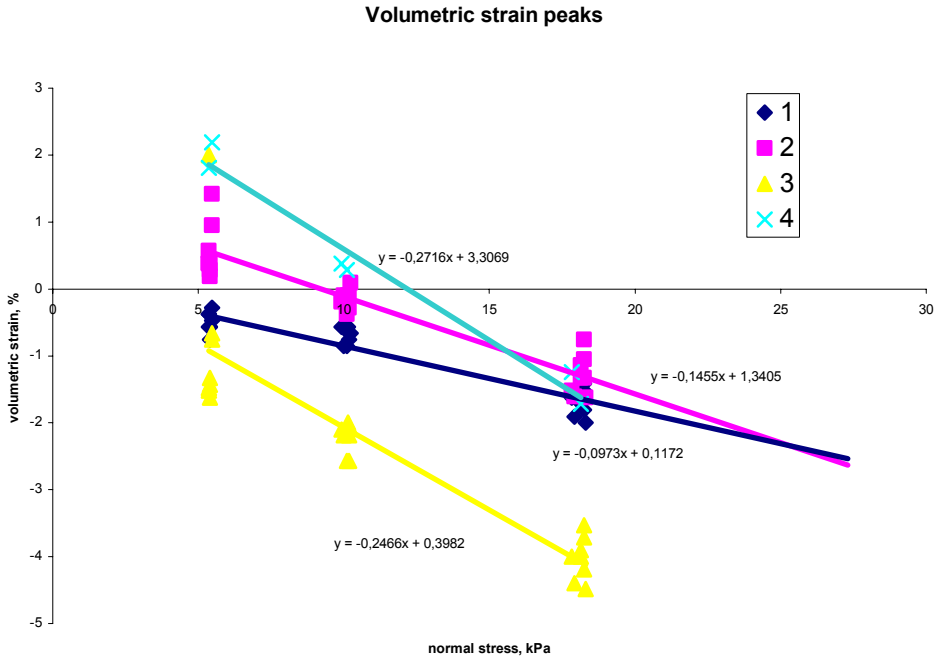

Figure 3.2.8: Graph of the heights of the volumetric strain curve versus the normal stress

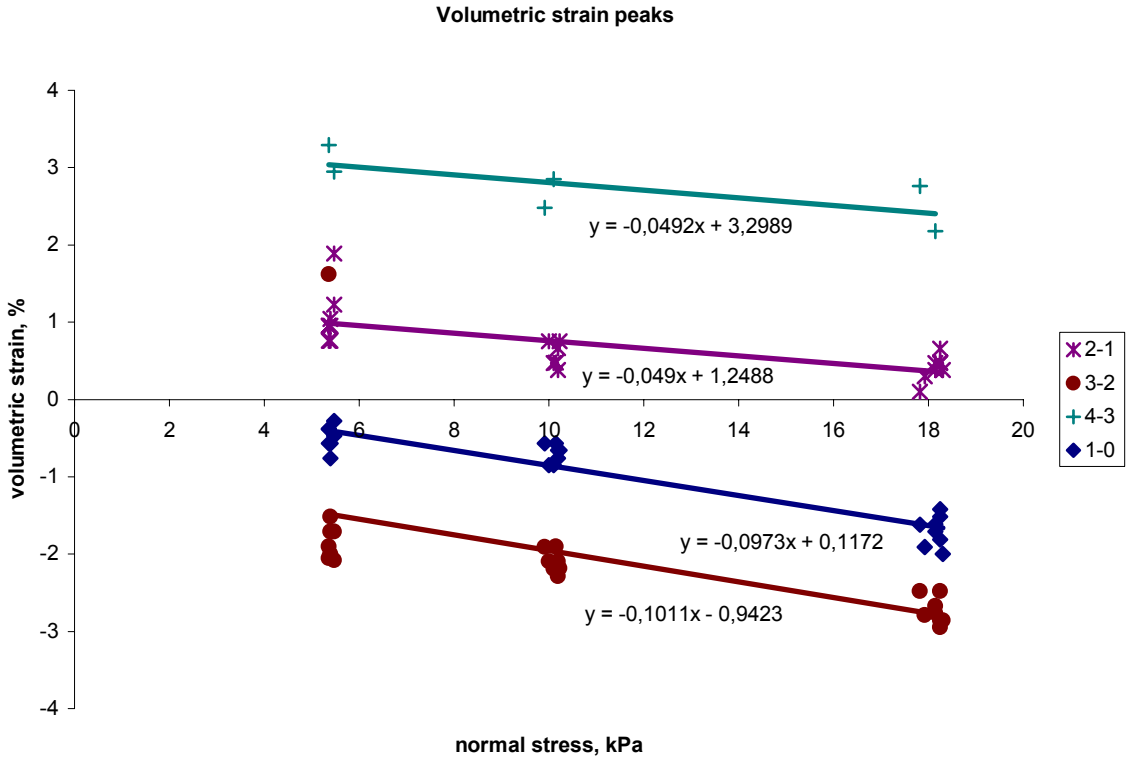

Figure 3.2.9: difference between volumetric strain peaks versus normal stress

3.2.2 Ring Shear Cell

The results from the Jenike Shear Cell show that stationary flow was not reached. To see how close the stationary flow was reached experiments are carried out with the Ring Shear Cell. With the Ring Shear Cell yield locus 4 and yield locus 5 are measured. Yield loci 2 and 3 could not be measured, because the applied stresses were too small for the device. In table 3.2.2 the stresses used during the experiments can be seen.

Table 3.2.2: normal stress at preshear (σ_{pr}) and the normal stress at shear (σ_{sh}) for yield loci 4 and 5

Yield locus	**σ_{pr} (kPa)**	**σ_{sh} (kPa)**
4	12.0	3.0
		4.8
		7.2
		9.6
5	24.0	6.0
		9.6
		14.4
		19.2

A couple of times the same series of experiments is done on the two yield loci. In appendix C the result for yield loci 4 and 5 are shown and in figure 3.2.10 and figure 3.2.11 a closer look is taken on the preshear peaks of the curves.

Although the measurements for each yield loci were carried out under the same circumstances, the results show a great diversity. At yield locus 4 even two kinds of tendencies in the curves can be distinguished. Measurements 294, 295 and 298 show a fast rise of the shear force, while measurements 300 and 308 show a more gradual rise of the shear force in time. Another remarkable thing is that the shear force at steady flow (or what seems steady flow) is very different for the different measurements. The steady flow seems to occur between 200 N and 300 N, which is a very broad range. But not only the first preshear peaks of every serie show an unpredictable behaviour. The shear curves for the different normal stresses applied also show this. Sometimes the preshear peaks appear later in the graph even exceed the peak of the first preshear peak.

For yield locus 5 the results seem a little better. But also here curves with a sharp increase of shear force occurred and also a broad range of shear force at steady flow is measured. The shear force here lies between 400 N and 450 N. To obtain reproducible results a consolidation procedure is needed.

The curves of the yield loci can be found in figure 3.2.12. Comparison between this figure and figure 3.2.2, which shows the yield loci measured with the Jenike Shear Cell, show that the slope of all curves are in the same range. In figure 3.2.13 yield locus 4 measured with the Jenike Shear Cell and the Ring Shear Cell are combined. It is clear from this picture that the slopes of the two curves are comparable, but also that the measured cohesion is very different for the devices used.

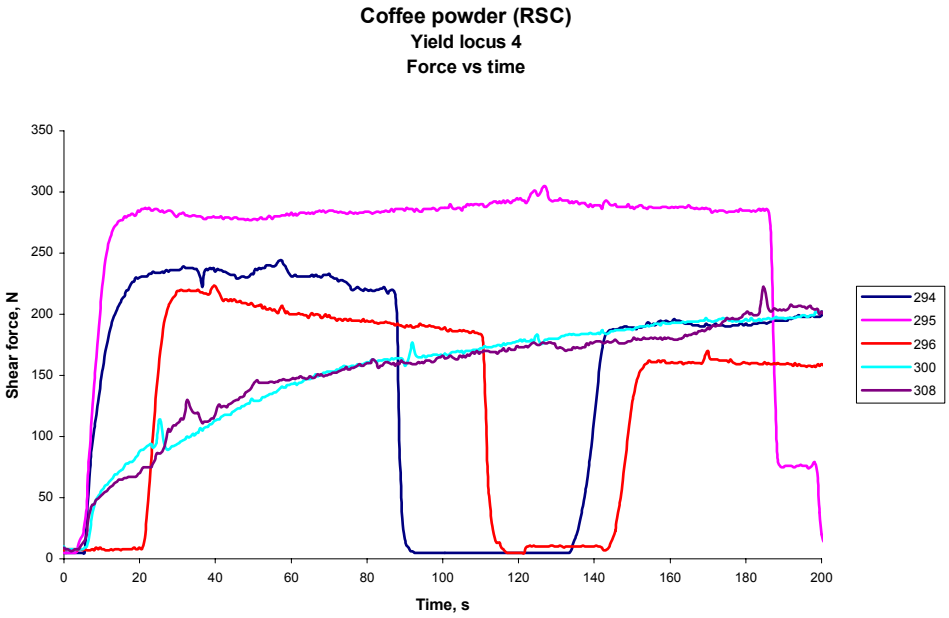

Figure 3.2.10: Shear force versus time at yield locus 4

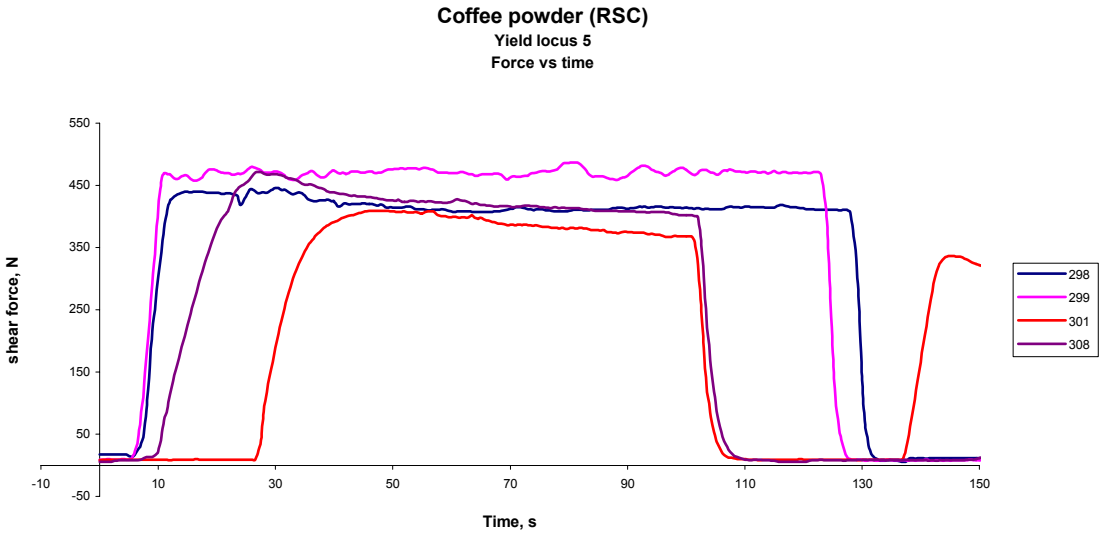

Figure 3.2.11: Shear force versus time at yield locus 5

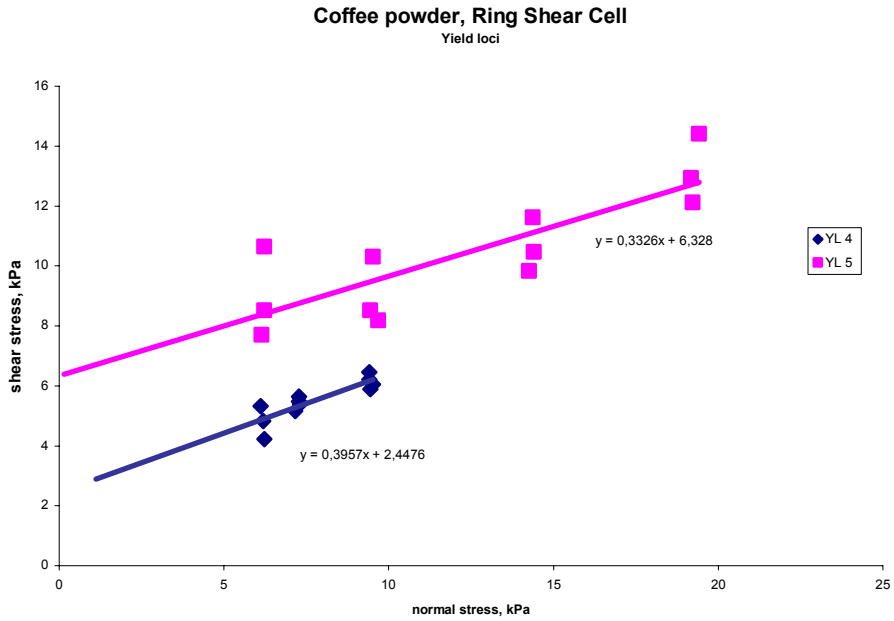

Figure 3.2.12: shear stress, τ, versus normal stress, σ, for the different yield loci of coffee powder with the Ring Shear Cell

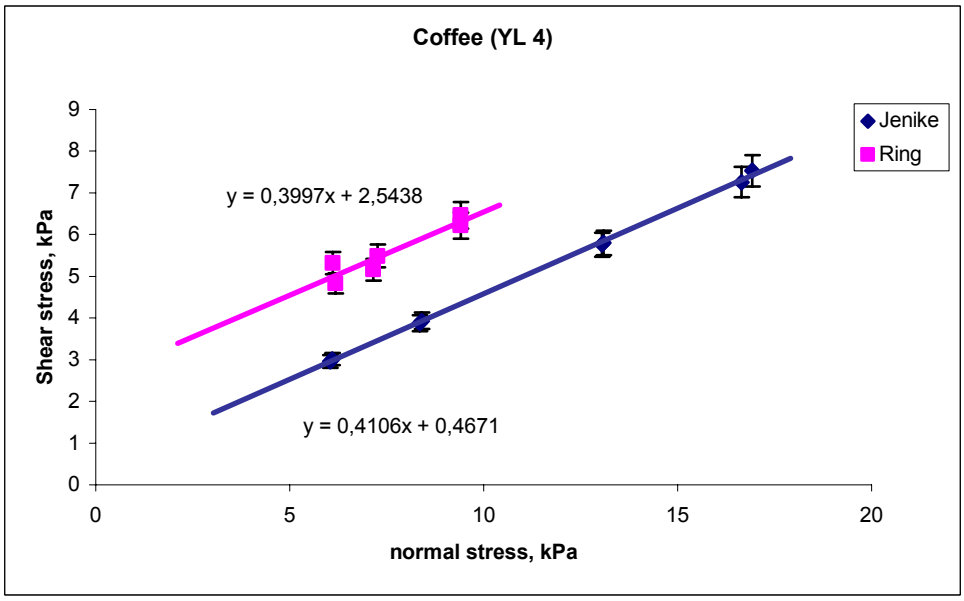

Figure 3.2.13: shear stress versus normal stress for yield locus 4

To compare the results of the Ring Shear Cell with the results of the Jenike Shear Cell the shear force is converted to shear stress divided by normal stress and plotted versus time for yield locus 4. In figure 3.3.14 the best curves are shown of the measurements with the Ring Shear Cell and also the average result of yield locus 4 of the Jenike Shear Cell. Measurement 300 with the Ring Shear Cell has a curve comparable to the curve of the Jenike Shear Cell, but it lies a little bit higher. The problem is the measurements are not reproducible and because of that hard to compare.
Because of the fact that the results of the Ring Shear Cell were not reproducible it was of no use to fit this data to a model as is done with the data of the Jenike Cell.

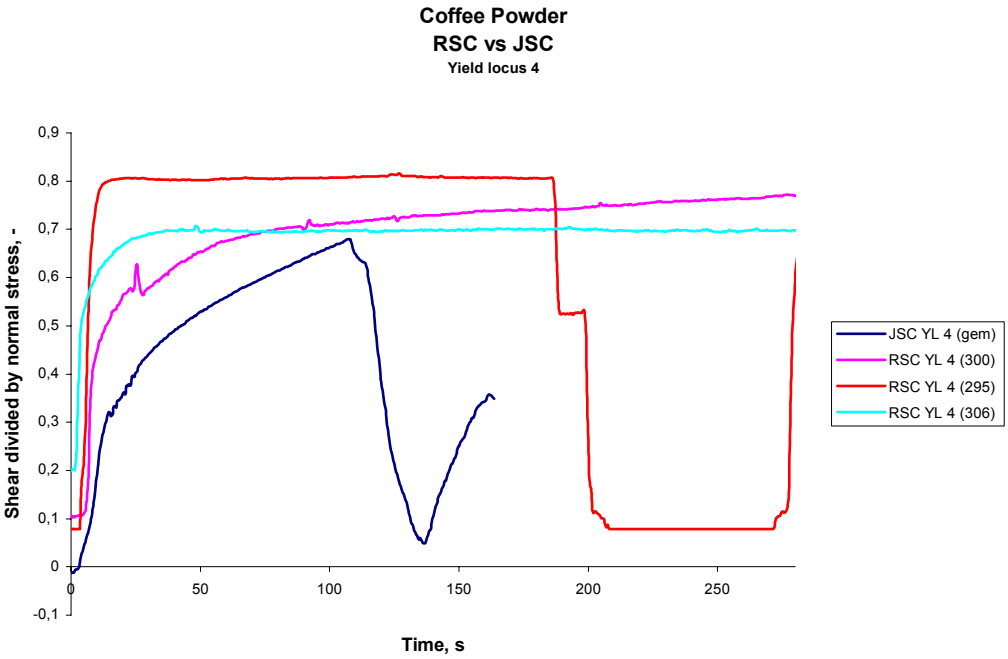

Figure 3.3.14: Shear stress divided by normal stress versus time at yield locus 4

4. Conclusion and recommendations

The goal of this project was to get more information about the flow behaviour of granular materials such as glass beads and coffee powder.
To determine if the particle size has an influence on the flow behaviour some experiments with glass beads were done. The analysis of the data obtained showed that the glass beads had a cohesion near zero, which means a that it is a free flowing material. (Visual examination and experience confirms this free flowing behaviour.) Further experiments, with mixed samples of monosize particle distributions, showed that there was no dependence on the particle size distribution of the flow behaviour for glass beads.

Knowing that the particle size distribution has no influence, some experiments were done with coffee powder. The results of the Jenike Shear Cell were difficult to analyse. One of the problems was that no stationary flow was reached during preshear. Because the shear curves are dependent on the fact that this stationary flow is reached the data of shear phase was quite useless for an analysis following the rules. Still some conclusions could be made, since the time during which preshear was applied on the sample was about the same for every measurement.

The graphs of the yield loci of coffee powder showed a curve with a slope of 0.4. This slope and the intersection of the yield locus with the y-axis depend on to what extent the stationary flow is reached. For every measurement this extent was different, so nothing can be said about the cohesion of the coffee powder. The data from the measurements with the Ring Shear Cell resulted in a curve of the yield locus with the same slope of 0.4. The intersection of the curves with the y-axis is totally different from those of the Jenike Shear Cell.
The preshear curves of the different Jenike measurements showed all a comparable increase of the shear force during time. This increase of shear force is fitted to the model $\tau/\sigma = c(x-x0)^{-A}$. For the parameters c and A a relation is obtained between the parameter and normal stress. For the parameter c this relation is $c=-0.0057\sigma+0.2472$ and for the parameter A it is $A=0.0037\sigma+0.2246$.
During the experiments also measurements were done on the height of the top of the shear cell. With respect to compression and dilatancy nothing strange was recorded, but also no tilt of the top was evidenced. During preshear and shear the density of the samples increased and during relaxation it decreased again.
One remarkable fact was that some of the shear force curves had a so called failure peak on a intermediate shear stress level. Comparison of several different possibilities for the cause of these peaks resulted in nothing. It is not clear why these peaks occur. One possible explanation is that it depends on the time during which consolidation is applied. Unfortunately this time is not recorded, but it would be an interesting experiment for the future.

The experiments with the Ring Shear Cell were carried out to see if the results obtained with the Jenike Shear Cell were close to the stationary flow. The results from the Ring Shear Cell were not reproducible for the different measurements. From the few measurements that looked reasonable, it seemed that the results of the Jenike Shear Cell and the Ring Shear Cell agreed with each other.
Due to the irreproducible results obtained with the Ring Shear Cell the data could not be fitted to a model and it could not be checked if the model used for the Jenike device was general enough to also describe the Ring Shear experiment.

Several things can have caused the bad results from the Ring Shear Cell. For example, no well defined preconsolidation was done with the Ring Shear Cell, which could explain the irreproducibility. Another influence on the data can be due to the top of the Cell. This top was very heavy and sometimes it dropped onto the sample or it was inclining to one side. Something else was the shear speed of the Ring Shear Cell. The cell was not always smoothly revolving, which resulted in little shocks and an uneven speed during the measurement. The dependence of the flow behaviour on the speed of the measurement would be something to investigate in the future.

In this research not very much reliable standard data is obtained due to what seems the changeability of the coffee powder. It is not yet clear if this changeability is caused by the chemical behaviour of the powder or due to the restrictions of the equipment used. One thing that would be really interesting is to combine a research on the physical chemistry of the coffee powder and the flow properties to see if and which properties of the powder change during the measurements.

5. Symbols

A	shear area
A_Z	shear area
D	diameter
d	distance
d*	distance at t=0
D_a	outer shear cell diameter
D_H	lever arm diameter
D_i	inner shear cell diameter
F_N	normal force
F_S	shear force
g	acceleration due to gravity
h_B	height of shear base
h_R	height of shear ring
h_T	inner height of shear base (RSC)
m_D	weight of cover
m_j	weight of joke/hanger
m_N	weight of the normal load
m_R	weight of the shear ring
V_B	volume of shear base
V_R	volume of shear ring
YL	Yield locus
ρ	density
σ	normal stress
$\sigma_{An,I}$	normal stress at preshear
$\sigma_{Ab,I}$	normal stress at shear
σ_C	consolidation stress
σ_{pr}	normal stress at preshear
σ_{sh}	normal stress at shear
τ	shear stress

6. Literature

[1] Patel H. and Karackattu J., *An analysis of the Flow Properties of Coffee Powder*, Technische Universiteit Delft and University of Florida
[2] Müller P., *Operating and Measuring Instructions for the Translational Shear Device (JENIKE shear cell)*, Otto-v.-Guericke-University Magdeburg, 2002
[3] *Practical course at powder flow properties and silo design*, Otto-v.-Guericke-University Magdeburg
[4] *Standard shear testing technique for particulate solids using the Jenike Shear Cell*, The institution of Chemical Engineers, 1989
[5] Rhodes M., *Introduction to Particle Technology*, John Wiley & Sons, 1998
[6] http://www.dietmar-schulze.de/grdle1.html